



<b>Title</b>	The extractability of potassium and radiocaesium in soils developed from granite and sedimentary rock in Fukushima, Japan
<b>Author(s)</b>	Ogasawara, Sho; Nakao, Atsushi; Eguchi, Tetsuya; Ota, Takeshi; Matsunami, Hisaya; Yanai, Junta; Shinano, Takuro
<b>Citation</b>	Journal of radioanalytical and nuclear chemistry, 323(1), 633-640 <a href="https://doi.org/10.1007/s10967-019-06971-2">https://doi.org/10.1007/s10967-019-06971-2</a>
<b>Issue Date</b>	2020-01
<b>Doc URL</b>	<a href="http://hdl.handle.net/2115/80114">http://hdl.handle.net/2115/80114</a>
<b>Rights</b>	This is a post-peer-review, pre-copyedit version of an article published in Journal of Radioanalytical and Nuclear Chemistry. The final authenticated version is available online at: <a href="http://dx.doi.org/10.1007/s10967-019-06971-2">http://dx.doi.org/10.1007/s10967-019-06971-2</a>
<b>Type</b>	article (author version)
<b>File Information</b>	Extractability_of_K_and_RCs (Final).pdf



[Instructions for use](#)

1 **Title Page**

2 Names of authors: Sho Ogasawara<sup>1,5</sup>, Atsushi Nakao<sup>1</sup>, Tetsuya Eguchi<sup>2</sup>, Takeshi

3 Ota<sup>3</sup>, Hisaya Matsunami<sup>2</sup>, Junta Yanai<sup>1</sup>, Takuro Shinano<sup>4</sup>

4 Title: Extractability of potassium and radiocaesium in soils developed from granite

5 and sedimentary rock in Fukushima, Japan

6 Affiliations and addresses of the authors:

7 <sup>1</sup> Graduate School of Life and Environmental Sciences, Kyoto Prefectural University,

8 Kyoto 606-8522, Japan

9 <sup>2</sup> Tohoku Agricultural Research Centre, NARO, Fukushima 960-2156, Japan

10 <sup>3</sup> Bio-oriented Technology Research Advancement Institution, NARO, 210-0005

11 Kanagawa, Japan

12 <sup>4</sup> Graduate School of Agriculture, Hokkaido University, Hokkaido 060-8589, Japan

13 <sup>e</sup> Japan Society for the Promotion of Science, 102-0083 Tokyo, Japan

14 E-mail address of the corresponding author:

15 Sho Ogasawara (shooga.0206@gmail.com)

16        **The extractability of potassium and radiocaesium in soils developed from**

17                                **granite and sedimentary rock in Fukushima, Japan**

18        Sho Ogasawara<sup>1,5</sup>, Atsushi Nakao<sup>1</sup>, Tetsuya Eguchi<sup>2</sup>, Takeshi Ota<sup>3</sup>, Hisaya

19                                Matsunami<sup>2</sup>, Junta Yanai<sup>1</sup>, Takuro Shinano<sup>4</sup>

20                                <sup>1</sup> *Graduate School of Life and Environmental Sciences, Kyoto Prefectural*

21    *University, 606-8522 Kyoto, Japan*

22                                <sup>2</sup> *Tohoku Agricultural Research Centre, NARO, 960-2156 Fukushima, Japan*

23                                <sup>3</sup> *Bio-oriented Technology Research Advancement Institution, NARO, 210-0005*

24    *Kanagawa, Japan*

25                                <sup>4</sup> *Graduate School of Agriculture, Hokkaido University, 060-8589 Hokkaido, Japan*

26                                <sup>5</sup> *Japan Society for the Promotion of Science, 102-0083 Tokyo, Japan*

27

28        **Abstract**

29        Potassium (K) and radiocaesium (RCs) were chemically extracted from soils derived

30        from granite (G soils) and sedimentary rock (S soils) in Fukushima, Japan. The

31 extractants employed were 1 M HNO<sub>3</sub>, concentrated HNO<sub>3</sub>, and HF + HClO<sub>4</sub>. As S  
32 soils contain a lower amount of trioctahedral 2:1 phyllosilicates than G soils, the  
33 RCs/K ratio was higher in S soils than in G soils with 1 M HNO<sub>3</sub> extraction,  
34 indicating that the potential risk of soil-to-plant transfer of RCs is higher in S soils  
35 than in G soils. In conclusion, information about surface geology is important in  
36 predicting the spatial pattern of soil characteristics related to transferability of RCs.

### 37 **Keywords**

38 agricultural soils, Fukushima prefecture, micaceous mineral, potassium,  
39 radiocaesium

### 40 **Introduction**

41 Phytoavailability of potassium (K) in soil is one of the most important factors in  
42 controlling the transfer of radiocaesium (RCs) from soil to plants. For the similar effective  
43 ionic radii of K and RCs, K competes with RCs at the ionic transporter in the root system  
44 [1, 2]. Therefore, uptake of RCs by plants is restricted in soils with a higher content of  
45 phytoavailable K, which is generally distinguished between exchangeable K [3–5] and  
46 nonexchangeable K [6, 7]. The exchangeable K is bound to soil components with weak

47 electrostatic power and can be thus absorbed readily by plants. In Fukushima prefecture,  
48 an exchangeable K content of  $>210 \text{ mg K kg soil}^{-1}$  is recommended to reduce transfer of  
49 RCs from the soil to plants based on the findings by Kato et al. [4]. Nonexchangeable K  
50 is retained more strongly in the soil and released more slowly than exchangeable K.  
51 Therefore, it is a secondary important reservoir of phytoavailable K, which can be utilized  
52 by plants once exchangeable K has been exhausted in the soil adjacent to the root surface  
53 (i.e., rhizosphere). Although little attention has been devoted to the effect of  
54 nonexchangeable K on the phytoavailability of RCs, recent research has shown that it is  
55 important in soils that have a low content of exchangeable K [7].

56 Nonexchangeable K is retained mainly in the interlayer of micaceous minerals (micas).  
57 As the interlayer site in mica can also adsorb RCs strongly, mica is considered to be a  
58 reservoir of both RCs and nonexchangeable K. Mica can be categorized into two types,  
59 i.e., trioctahedral mica (e.g., biotite) and dioctahedral mica (e.g., illite), based on the  
60 number of metal cations occupying the octahedral structure. Trioctahedral mica is known  
61 to be able to release its interlayer  $\text{K}^+$  more readily than the dioctahedral mica [8]. Which  
62 of the two types is dominant in a particular soil is highly relevant to surface geology. In  
63 the eastern Fukushima prefecture, surface geology can be divided into granite and

64 sedimentary rock [9]. Biotite is dominant in soils derived from granite (G soils) [10],  
65 whereas illite is dominant in soils derived from sedimentary rock (S soils) [11]. Given the  
66 relevance of geology to soil mineralogy, it is very likely that G soils have a higher  
67 nonexchangeable K content than S soils and, therefore, a lower risk of soil-to-plant  
68 transfer of RCs. Few studies in Fukushima prefecture evaluated the difference in the  
69 nonexchangeable K content of soils with different geological backgrounds. Therefore,  
70 this study aims to investigate the relative abundance of di- or trioctahedral minerals in  
71 soils in Fukushima prefecture and clarify the relationship between the mineralogy and  
72 extractability of K and RCs from soils with different geological backgrounds.

### 73 **Materials**

74 Twenty-eight soil samples were collected at depths of 0–10 cm from 14 agricultural  
75 fields in granitic areas (sample names: G1–G14) and 14 fields in sedimentary rock  
76 areas (S1–S14) in Fukushima prefecture. The G12 and G13 soils were sampled from  
77 a buckwheat field and from pasture, respectively. The remaining soil samples were  
78 collected from paddy fields, including fallow fields. Surface geology was assessed  
79 on the basis of the surface geology map produced by AIST [9]. The sampling  
80 locations and the geology map are shown in Fig. 1. This sample set did not include

81 decontaminated soils because the decontamination procedure generally involves  
82 applying uncontaminated soil brought from other areas [12]. The soil samples were  
83 air-dried and sieved using  $\leq 2$ -mm mesh. During sieving, as many plant residues as  
84 possible were removed using tweezers.

## 85 **Experimental**

### 86 **1. Mineralogical analysis**

87 The types of phyllosilicate minerals, di- and/or trioctahedral, contained in the soil  
88 were distinguished by (060) reflections of powdered X-ray diffraction (XRD)  
89 analysis (SmartLab-FE, Rigaku, Tokyo, Japan,  $\text{CuK}\alpha$  radiation). A 3-g portion of  
90 soil was suspended in water via ultrasonic treatment, and wet sieving and freeze-  
91 drying were used to collect the clay–silt fraction (particle diameter  $\leq 20$   $\mu\text{m}$ ) in the  
92 soil. The dried particles were ground softly using a ceramic pestle and mortar.  
93 Removal of organic matter and iron oxides, which are standard pretreatments for  
94 XRD analysis of soils' clays, was avoided because these treatments alter the structure  
95 of iron-bearing 2:1 clay minerals via either oxidative or reductive reactions [13]. A  
96 portion of the powdered clay–silt fraction was oriented randomly on a glass slide and  
97 scanned from  $59^\circ$  to  $63^\circ$   $2\theta$ , with steps of  $0.0050^\circ$   $2\theta$  and a scan speed of  $0.1^\circ$   $2\theta$

98  $\text{min}^{-1}$ . Areas of the diffraction peaks recorded were quantified by decomposition into  
99 a Lorentzian-shaped peak using PeakFit software ver. 4.12 (SeaSolve Software Inc.,  
100 Framingham, MA).

## 101 **2. Chemical extractions**

102 Potassium and RCs were extracted from soils using three methods: hot 1 M nitric  
103 acid ( $\text{HNO}_3$ ) extraction (Ex. 1), concentrated  $\text{HNO}_3$  extraction (Ex. 2), and residue  
104 decomposition (Ex. 3). The Ex. 1 was almost the same as the extraction procedure  
105 for phytoavailable K in soil [14]. The Ex. 2 was the modified method of the “strong  
106 acid dissolution” by Saito et al. [15]. The Ex. 3 was the decomposition of the residue  
107 that remained after the Ex. 2 using hydrofluoric acid (HF) and perchloric acid  
108 ( $\text{HClO}_4$ ).

109 Ex. 1 (hot 1 M  $\text{HNO}_3$  extraction): A 10-g portion of soil and 100 mL of 1 M  $\text{HNO}_3$   
110 were mixed in a 200-mL Erlenmeyer flask and preheated on a hotplate for 20 min  
111 until boiling and then heated for a further 15 min. After heating, the flask was allowed  
112 to cool for 5 min at room temperature, and the suspension was filtered using filter  
113 paper. The residue on the filter paper was washed using 0.1 M  $\text{HNO}_3$ . The filtrate



114 was then filtered using a 0.45- $\mu\text{m}$  syringe filter and brought up to 100 mL with 0.1  
115 M  $\text{HNO}_3$ .

116 Ex. 2 (concentrated  $\text{HNO}_3$  extraction): A 5-g portion of soil and 25 mL 13.4 M  $\text{HNO}_3$   
117 (density = 1.38) were mixed in a Teflon beaker and heated on a hotplate for 3 h at  
118 100°C. After heating, the suspension was diluted with ultrapure water, centrifuged  
119 to recover the residue, and filtered using a 0.45- $\mu\text{m}$  syringe filter. The filtrate was  
120 brought up to 100 mL with pure water. The residue was dried in an oven overnight  
121 at 105°C.

122 Ex. 3 (digestion of residue): The dried residue was powdered using a tungsten carbide  
123 pestle and mortar. A 0.5-g portion of powdered soil was weighed into a Teflon beaker  
124 and digested using HF and  $\text{HClO}_4$  while being heated on a hotplate. The decomposed  
125 products were dissolved using hydrogen chloride and  $\text{HNO}_3$  and brought up to 50  
126 mL.

127 The above extractions were performed in duplicate. The Ex. 1 and Ex. 2 were  
128 performed independently, and not subsequently, to obtain higher concentrations of  
129 RCs in the extracted solution for more precise radiometric analyses. The amount of  
130 K and RCs extracted using Ex. 1 was denoted as fraction 1 (F1). The fraction 2 (F2)

131 was calculated by subtracting the amounts of K or RCs in the Ex.1 solutions from  
132 those in the Ex. 2 solutions. The amount of K and RCs extracted using Ex. 3 was  
133 denoted as fraction 3 (F3).

### 134 **3. Quantification of K and RCs**

135 The K concentrations in the Ex. 1, Ex. 2, and Ex. 3 solutions were determined using  
136 atomic absorption spectrometry (ZA-3000, Hitachi High-Technologies Corporation,  
137 Tokyo, Japan). The RCs dissolving in the Ex. 1 and Ex. 2 solutions were concentrated  
138 via the ammonium phosphomolybdate (AMP) method [16] and determined using a  
139 sodium iodide (NaI) scintillation counter (2480 WIZARD<sup>2</sup>, Perkin Elmer, MA,  
140 USA), with a relative standard deviation (RSD) of <5 %. The AMP has a strong  
141 ability to adsorb Cs<sup>+</sup> and has low solubility in water and particularly in nitric acid  
142 [17]; therefore, RCs in the acidic solution can be concentrated and recovered as an  
143 AMP-Cs compound. As described in detail by Aoyama and Hirose [16],  
144 approximately 0.2 g of AMP was added to the Ex. 1 and Ex. 2 solutions and stirred  
145 with a magnetic stirrer for 1 h, and the AMP-Cs compound was recovered on the  
146 next day using the 0.45- $\mu$ m filter. The collected AMP-Cs compound was dissolved  
147 using 2 mL of 1 M sodium hydroxide in a 75-mm-long polypropylene tube with a

148 12-mm radius for geometry matching, and the RCs content was measured using an  
149 NaI scintillation counter (2480 WIZARD<sup>2</sup>, Perkin Elmer, MA, USA), with an RSD  
150 of <5 %. The RCs concentrations in the Ex. 3 solutions were not determined directly,  
151 but the RCs concentration in F3 was calculated by subtracting those in F1 and F2  
152 from the total RCs concentration in the soil. The total RCs concentration in soil was  
153 calculated from the total concentration of <sup>137</sup>Cs in soil and the half-life of <sup>137</sup>Cs (30.1  
154 y) and <sup>134</sup>Cs (2.07 y) assuming that RCs is the sum of <sup>137</sup>Cs and <sup>134</sup>Cs and that the  
155 <sup>137</sup>Cs/<sup>134</sup>Cs activity ratio was 1.0 at the time of the Fukushima Dai-ichi Nuclear  
156 Power Plant accident [18]. The total <sup>137</sup>Cs concentration in soil was determined using  
157 the Ge semiconductor detector (GC2520, Canberra, Meriden, CT, USA), with an  
158 RSD of <5%.

## 159 **Results and Discussions**

### 160 **1. Mineralogy of soil samples**

161 The XRD patterns at 59–63 °2θ of the clay–silt fraction from G and S soils are shown  
162 in Fig. 2. All the samples exhibited four prominent peaks at approximately 59.9 °2θ,  
163 60.1 °2θ, 61.8 °2θ, and 62.3 °2θ, corresponding to the presence of quartz (Qz),  
164 trioctahedral mineral (Tri), dioctahedral mineral (Di), and kaolinite (Kl), respectively

165 [19]. The peak positions for Tri and Qz and those for Di and Kl were close enough  
166 to overlap with each other. The G soils exhibited prominent Tri peaks, but they  
167 exhibited a very small Di peak that was nearly concealed by the adjacent large Kl  
168 peaks, suggesting that these soils were enriched with trioctahedral phyllosilicates. In  
169 contrast, most of the S soils exhibited a prominent Di peak together with a distinct  
170 Tri peak, suggesting that these soils contained both di- and trioctahedral  
171 phyllosilicates. Trioctahedral phyllosilicates in the S soils may have been transported  
172 there by streams running through granite in the uplands.

173 Table 1 shows the peak areas of Tri and Di. The peak areas in the powder XRD may  
174 vary depending on the amount of sample oriented on glass slides. Hence, we  
175 determined the ratios of Tri peak areas against the sum of the Tri and Di peak areas  
176 ( $\text{Tri}/(\text{Di}+\text{Tri})$ ) as a quantitative indicator of the relative abundance of trioctahedral  
177 phyllosilicates. For G soils, the average value of  $\text{Tri}/(\text{Di}+\text{Tri})$  was 0.72, whereas it was  
178 0.43 for S soils. The  $\text{Tri}/(\text{Di}+\text{Tri})$  values for G soils were significantly higher ( $P <$   
179  $0.01$ ) than those for S soils, which is a direct indication that the G soils contained a  
180 higher amount of trioctahedral minerals than the S soils. Relatively low  $\text{Tri}/(\text{Di}+\text{Tri})$

181 values for G5, G11, and G12 also corresponded with the presence of Di peaks in their  
182 XRD patterns (Fig. 2).

## 183 **2. The extractability of RCs and K**

184 Individual data on the extractability of K and RCs from soils are presented in Table  
185 2, and their summary data are shown as boxplots in Fig. 3 and Fig. 4, respectively.

186 For G soils, the medians of K extractability were 5.0% in F1, 13.3% in F2, and 82.5%  
187 in F3, whereas those for S soils were 2.7% in F1, 2.6% in F2, and 94.9% in F3. In G  
188 soils, the K extractability in F1 and F2 was significantly higher than that in S soils,  
189 confirming that the phytoavailable K content in G soils is higher than that in S soils.

190 However, even in G soils, the K extractability of G soils with Di peaks (G5, G11,  
191 and G12) was relatively low. The K extractability for G5, G11, and G12 in F1 were  
192 1.4%, 2.3%, and 3.0 %, respectively, and the corresponding values in F2 were 2.9%,  
193 6.3%, and 7.7%, respectively (Table 2). These values were lower than the medians  
194 of K extractability for G soils, indicating lower contribution of dioctahedral mica to  
195 the K supply.

196 For G soils, the medians of extractability of RCs were 20.4% in F1, 16.8% in F2, and  
197 61.7% in F3, whereas those for S soils were 25.6% in F1, 28.6% in F2, and 44.6% in

198 F3. In contrast to those of K, the medians of extractability of RCs in F1 and F2 for  
199 G soils were lower than those for S soils and the extractability of RCs in F3 for G  
200 soils was significantly higher than that for S soils. This higher persistence in F3 for  
201 G soils may be linked to these soils having a larger amount of fixation sites for RCs  
202 than is the case with S soils. Fixation of RCs in soil occurs on the weathered edge of  
203 mica, known as the frayed edge site (FES) [20]; Ogasawara et al. [7] showed that S  
204 soils had lower FES content than G soils. A higher FES content in soil is responsible  
205 for the lower extractability of RCs by ammonium ions ( $\text{NH}_4^+$ ) [7, 21, 22] and by 0.1  
206 M hydrochloric acid [22] while these methods extract RCs adsorbed on soil more  
207 weakly than extractions performed in this study. The effect of the FES content in soil  
208 on the strength of the adsorption of RCs should be examined further.

### 209 **3. RCs uptake risk assessment based on the extractability of RCs and K**

210 Kondo et al. [23] reported that the relative extractability of  $^{137}\text{Cs}$  to K by  $\text{NH}_4^+$  was  
211 proportional to the concentration of  $^{137}\text{Cs}$  in plants, indicating that higher  
212 extractability of RCs and/or lower extractability of K results in a higher uptake of  
213 RCs by plants. In addition, in the current study, we calculated the relative  
214 extractability of RCs to K (RCs/K) was calculated to assess the risk of uptake of RCs

215 by plants (Table 3). These summary data are presented as a boxplot in Fig. 5. The  
216 median values of RCs/K for G soils were 3.7 in F1, 1.3 in F2, and 0.8 in F3, whereas  
217 the values for S soils were 9.6 in F1, 12.5 in F2, and 0.5 in F3. The RCs/K value for  
218 G soils was significantly lower than that for S soils in F1 ( $P < 0.05$ ) and F2 ( $P <$   
219  $0.001$ ), and the RCs/K value in F3 for G soils was significantly higher ( $P < 0.01$ )  
220 than that for S soils, indicating that G soils have a lower risk of transfer of RCs than  
221 S soils. This finding corresponds with those of previous studies reported that uptake  
222 of RCs by rice in granite areas was smaller than that in sedimentary rock areas [7,  
223 24]. Moreover, RCs/K values in F1 were negatively correlated ( $P < 0.001$ ) with  
224 Tri/Di+Tri values (Fig. 6). This relationship indicated that soils containing more  
225 trioctahedral minerals have lower risk of RCs uptake by plants. Although most of the  
226 G soils were plotted in the lower-right area, G soils with a Di peak, especially G5  
227 and G 11, were plotted in the upper-left area. This indicated that some G soils have  
228 lower trioctahedral mineral contents and, hence, have a higher risk of uptake of RCs  
229 by plants. Therefore, use of XRD analysis data as supporting information for surface  
230 geology would be an effective and more reliable method to estimate the relative risk  
231 of transfer of RCs from soils to plants.

232           **Conclusion**

233    The effect of mica type, either trioctahedral mica or dioctahedral mica, in soil on the  
234    extractability of K and RCs was examined using G soils and S soils. The release of  
235    more K and less RCs from G soils than from S soils demonstrated that the risk of  
236    uptake of RCs by plants is potentially lower in G soils than in S soils. Though surface  
237    geology is useful in estimating whether either trioctahedral mica or dioctahedral mica  
238    is dominant in the soil, some soils in granite areas can have relatively lower contents  
239    of trioctahedral minerals. The combined use of surface geology information and  
240    XRD analysis would be a more effective and reliable approach for estimating the risk  
241    of transfer of RCs from soils to plants.

242           **Acknowledgments**

243    Gratitude is expressed to the Food Safety and Consumer Affairs Bureau, MAFF, prof.  
244    Shin Moono (Faculty of Food and Agricultural Sciences, Fukushima University), Dr.  
245    Yuzo Manpuku (Institute for Agro-Environmental Sciences, NARO), Dr. Tomoaki  
246    Nemoto (Fukushima Prefectural Government), Dr. Takashi Saito (same as above), Mr.  
247    Kazuhiro Kohata (same as above), and the agricultural department of Minamisoma city  
248    and Namie town who helped soil samples collection. Authors also appreciate Ms. Yuko



249 Abe (Tohoku Agricultural Research Centre, NARO) for the help of experiments. The  
250 authors would like to thank Enago (www.enago.jp) for the English language review.  
251 Analyses of RCs measurements were carried out in the Laboratory of Radioisotopes of  
252 Kyoto Prefectural University.

### 253 **Funding**

254 This work was financially supported by the JSPS KAKENHI [grant number  
255 JP15J06569 and 16H06188].

### 256 **References**

- 257 1. Smolders E, Van Den Brande K, Merckx R (1997) Concentrations of  $^{137}\text{Cs}$  and K in  
258 soil solution plant availability of  $^{137}\text{Cs}$  in soils. *Environ Sci Technol.* 31, 12:  
259 3432–3438
- 260 2. White PJ, Broadley MR (2000) Mechanisms of caesium uptake by plants. *New*  
261 *Phytol.* 147, 2: 241–256
- 262 3. MAFF (2014) Causes of contamination by radiocesium and countermeasures for  
263 these problems. *Minist Agric For Fish.* 0–24

- 264 4. Kato N, Kihou N, Fujimura S, Ikeba M, Miyazaki N, Saito Y, Eguchi T, Itoh S  
265 (2015) Potassium fertilizer and other materials as countermeasures to reduce  
266 radiocesium levels in rice: Results of urgent experiments in 2011 responding to  
267 the Fukushima Daiichi Nuclear Power Plant accident. *Soil Sci Plant Nutr.* 61:  
268 179–190
- 269 5. Kubo K, Fujimura S, Kobayashi H, Ota T, Shinano T (2017) Effect of soil  
270 exchangeable potassium content on cesium absorption and partitioning in  
271 buckwheat grown in a radioactive cesium-contaminated field. *Plant Prod Sci.*  
272 2017.
- 273 6. Eguchi T, Ohta T, Ishikawa T, Matsunami H, Takahashi Y, Kubo K, Yamaguchi N,  
274 Kihou N, Shinano T (2015) Influence of the nonexchangeable potassium of mica  
275 on radiocesium uptake by paddy rice. *J Environ Radioact.* 147: 33–42
- 276 7. Ogasawara S, Eguchi T, Nakao A, Fujimura S, Takahashi Y, Matsunami H, Tsukada  
277 H, Yanai J, Shinano T (2019) Phytoavailability of <sup>137</sup>Cs and stable Cs in soils  
278 from different parent materials in Fukushima, Japan. *J Environ Radioact.* 198:  
279 117–125

- 280 8. Fanning D, Keramidas V, El-Deskoy M (1989) Micas. In: Dixon JB, Weed SB (Eds.),  
281 Minerals in Soil Environments, Soil Sci Soc Am, Madison, 551–634
- 282 9. AIST (ed.), Geological Survey of Japan 2014. Seamless digital geological map of Japan  
283 1: 200,000. Jan 14, 2014 version, Geological Survey of Japan, National Institute of  
284 Advanced Industrial Science and Technology
- 285 10. Mukai H, Hatta T, Kitazawa H, Yamada H, Yaita T, Kogure T (2014) Speciation of  
286 radioactive soil particles in the Fukushima contaminated area by IP  
287 autoradiography and microanalyses. *Environ Sci Technol.* 48, 22: 13053–13059
- 288 11. Ramseyer K, Boles JR (1986) Mixed-layer illite/smectite minerals in tertiary  
289 sandstones and shales, San Joaquin Basin, California. *Clays Clay Miner.* 34, 2:  
290 115–124
- 291 12. Fukushima Prefectural Government, 2018  
292 <http://www.pref.fukushima.lg.jp/site/portal-english/en02-03.html> (accessed on  
293 Aug. 20, 2019)
- 294 13. Ross GJ, Rich CI (1974) Effect of oxidation and reduction on potassium exchange  
295 of biotite. *Clays Clay Miner.* 22, 4: 355–360

- 296 14. Helmke PA, Sparks DL (1996) Lithium, Sodium, Potassium, Rubidium, and Cesium.  
297 In: Sparks, D. L. (Ed.), *Methods of soil analysis Part 3—Chemical methods*, SSSA  
298 Book Series. no. 5, Madison, WI, 560–563.
- 299 15. Saito T, Makino H, Tanaka S (2014) Geochemical and grain-size distribution of  
300 radioactive and stable cesium in Fukushima soils: Implications for their long-  
301 term behavior. *J Environ Radioact.* 138: 11–18
- 302 16. Aoyama M, Hirose K (2008) Radiometric determination of anthropogenic  
303 radionuclides in seawater. *Radioact Environ.* 11: 137–162
- 304 17. Budavari S, O’Neil MJ, Smith A, Heckelman PE, Kinneary JF (Eds) (1996) *The*  
305 *Merck Index, An Encyclopedia of Chemicals, Drugs, and Biologicals* (12th  
306 ed.). Merck & Co., Inc., New Jersey, 589
- 307 18. Hirose K (2012) 2011 Fukushima Dai-ichi nuclear power plant accident: Summary  
308 of regional radioactive deposition monitoring results. *J Environ Radioact.* 111:  
309 13–17
- 310 19. Moore DM, Reynolds RC Jr. (1997) Identification of clay minerals and associated  
311 minerals, In: *X-ray diffraction and the identification and analysis of clay minerals*  
312 (Second Edition). Oxford University Press, Madison, NY, 227–260.

- 313 20. Sawhney BL (1972) Selective sorption and fixation of cations by clay minerals: A  
314 review. *Clays Clay Miner.* 20: 93–100
- 315 21. Delvaux B, Kruyts N, Cremers A (2000) Rhizospheric mobilization of radiocesium  
316 in soils. *Environ Sci Technol.* 34, 8: 1489–1493
- 317 22. Vandebroek L, Hees MV, Delvaux B, Spaargaren O, Thiry Y (2012) Relevance of  
318 radiocaesium interception potential (RIP) on a worldwide scale to assess soil  
319 vulnerability to <sup>137</sup>Cs contamination. *J Environ Radioact.* 104: 87–93
- 320 23. Kondo M, Maeda H, Goto A, Nakano H, Kiho N, Makino T, Sato M, Fujimura S,  
321 Eguchi T, Hachinohe M, Hamamatsu S, Ihara H, Takai T, Arai-Sanoh Y, Kimura  
322 T (2015) Exchangeable Cs/K ratio in soil is an index to estimate accumulation of  
323 radioactive and stable Cs in rice plant. *Soil Sci Plant Nutr.* 61: 133–143
- 324 24. Yamamura K, Fujimura S, Ota T, Ishikawa T, Saito T, Arai Y, Shinano T (2018) A  
325 statistical model for estimating the radiocesium transfer factor from soil to brown  
326 rice using the soil exchangeable potassium content. *J Environ Radioact.* 195:  
327 114–125
- 328

329 **Table 1** Peak areas of tri- (Tri) and dioctahedral minerals (Di) contained in (a) G  
 330 soils and (b) S soils and the peak area ratio of trioctahedral minerals against the sum  
 331 of di- and trioctahedral minerals.

(a)				(b)			
Sample name	Peak area		Tri/Di+Tri	Sample name	Peak area		Tri/Di+Tri
	Tri	Di			Tri	Di	
G1	1490	1120	0.57	S1	930	2410	0.28
G2	1910	809	0.70	S2	776	2160	0.26
G3	3050	583	0.84	S3	596	2190	0.21
G4	1910	267	0.88	S4	647	2310	0.22
G5	1030	1620	0.39	S5	1270	1590	0.44
G6	2940	681	0.81	S6	2340	1110	0.68
G7	1620	380	0.81	S7	1800	494	0.78
G8	1170	473	0.71	S8	715	261	0.73
G9	2470	729	0.77	S9	2330	1590	0.59
G10	1350	597	0.69	S10	1130	5540	0.17
G11	1080	1380	0.44	S11	2020	1760	0.53
G12	1230	1040	0.54	S12	1920	1580	0.55
G13	1850	42.8	0.98	S13	1770	5240	0.25
G14	1630	158	0.91	S14	872	2100	0.29
average	1770	706	0.72	average	1370	2170	0.43

333

334 **Table 2** Extractability of K and RCs for G soils and S soils

sample name	K extractability						RCs extractability							
	F1		F2		F3		Total	F1		F2		F3		Total
	(g kg <sup>-1</sup> )	(%)	(g kg <sup>-1</sup> )	(%)	(g kg <sup>-1</sup> )	(%)		(Bq kg <sup>-1</sup> )	(%)	(Bq kg <sup>-1</sup> )	(%)	(Bq kg <sup>-1</sup> )	(%)	
G1	0.71	6.6	0.64	6.0	9.4	87	10.8	220	23	130	14	610	64	960
G2	1.14	5.2	2.10	10	18.6	85	21.9	370	34	120	11	610	55	1100
G3	0.63	3.1	2.20	11	17.9	86	20.8	330	24	380	27	690	49	1400
G4	0.98	5.3	2.79	15	14.8	80	18.6	450	26	490	29	760	45	1700
G5	0.37	1.4	0.78	2.9	25.6	96	26.7	1700	31	900	17	2800	52	5400
G6	1.69	12	3.63	25	9.2	63	14.5	260	20	170	13	870	67	1300
G7	0.76	5.6	3.00	22	9.8	72	13.6	320	17	370	19	1200	63	1900
G8	0.80	4.8	2.95	18	12.8	77	16.5	190	11	450	26	1100	65	1700
G9	1.43	8.4	5.08	30	10.5	62	17.1	220	17	190	15	890	68	1300
G10	0.80	4.7	3.58	21	12.8	74	17.2	220	18	160	13	820	68	1200
G11	0.55	2.3	1.52	6.3	22.0	91	24.1	220	22	170	17	610	61	1000
G12	0.75	3.0	1.92	7.7	22.4	89	25.0	140	10	110	8	1200	86	1400
G13	2.01	13	4.85	32	8.3	55	15.1	430	18	550	23	1400	58	2400
G14	0.93	3.0	3.57	12	26.1	85	30.6	29000	21	55000	39	56000	40	140000
S1	0.43	2.6	0.19	1.2	15.6	96	16.3	990	29	810	24	1600	47	3400
S2	0.55	3.9	0.48	3.4	12.9	93	13.9	2300	29	2400	31	3100	40	7800
S3	0.32	2.7	0.31	2.6	11.1	95	11.7	1100	30	1200	32	1400	38	3700
S4	0.46	3.9	0.37	3.1	11.0	93	11.8	520	20	780	30	1300	50	2600
S5	0.74	4.4	1.05	6.2	15.0	89	16.8	11000	25	12000	27	21000	48	44000
S6	0.24	1.1	0.13	0.6	21.3	98	21.6	150	10	370	25	980	65	1500
S7	0.42	2.6	0.35	2.2	15.3	95	16.1	150	8	520	27	1200	63	1900
S8	0.53	2.8	0.15	0.8	18.2	96	18.8	230	15	230	15	1000	67	1500
S9	0.88	5.5	1.13	7.1	14.0	87	16.0	380	25	370	25	750	50	1500
S10	0.26	1.1	0.37	1.6	22.4	97	23.0	310	26	400	33	490	41	1200
S11	0.53	2.8	0.91	4.8	17.3	92	18.8	410	29	460	33	530	38	1400
S12	0.53	2.8	1.28	6.7	17.4	91	19.2	530	33	470	29	600	38	1600
S13	0.33	1.4	0.60	2.5	22.5	96	23.4	270	23	490	41	440	37	1200
S14	0.40	2.0	0.44	2.2	19.2	96	20.0	570	30	530	28	800	42	1900

335

336

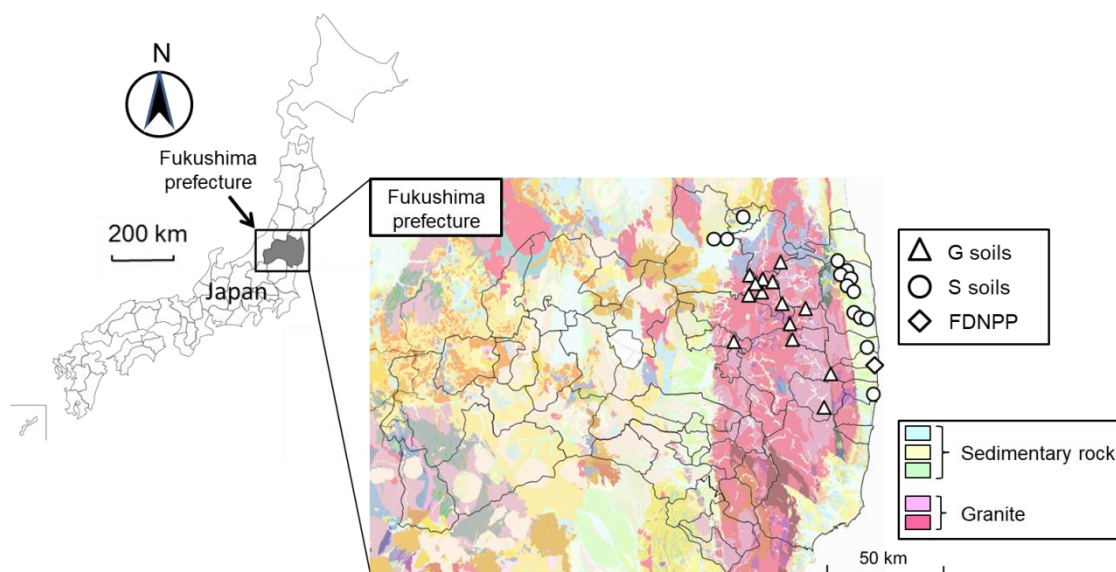
337 **Table 3** Relative extractability of RCs to K

sample name	RCs/K			
	F1	F2	F3	
G soils	G1	3.4	2.3	0.73
	G2	6.4	1.1	0.65
	G3	7.7	2.6	0.57
	G4	5.0	1.9	0.56
	G5	23	5.7	0.54
	G6	1.7	0.5	1.06
	G7	3.0	0.9	0.87
	G8	2.3	1.5	0.84
	G9	2.0	0.5	1.1
	G10	3.9	0.6	0.92
	G11	9.6	2.7	0.67
	G12	3.3	1.0	0.96
	G13	1.4	0.7	1.1
	G14	6.8	3.4	0.47
S soils	S1	11	20	0.49
	S2	7.5	9.0	0.43
	S3	11	12	0.40
	S4	5.2	9.6	0.54
	S5	5.7	4.4	0.53
	S6	8.9	41	0.66
	S7	3.0	13	0.66
	S8	5.5	19	0.69
	S9	4.6	3.5	0.57
	S10	23	21	0.42
	S11	10	6.8	0.41
	S12	12	4.4	0.41
	S13	16	16	0.38
	S14	15	13	0.44

338

339

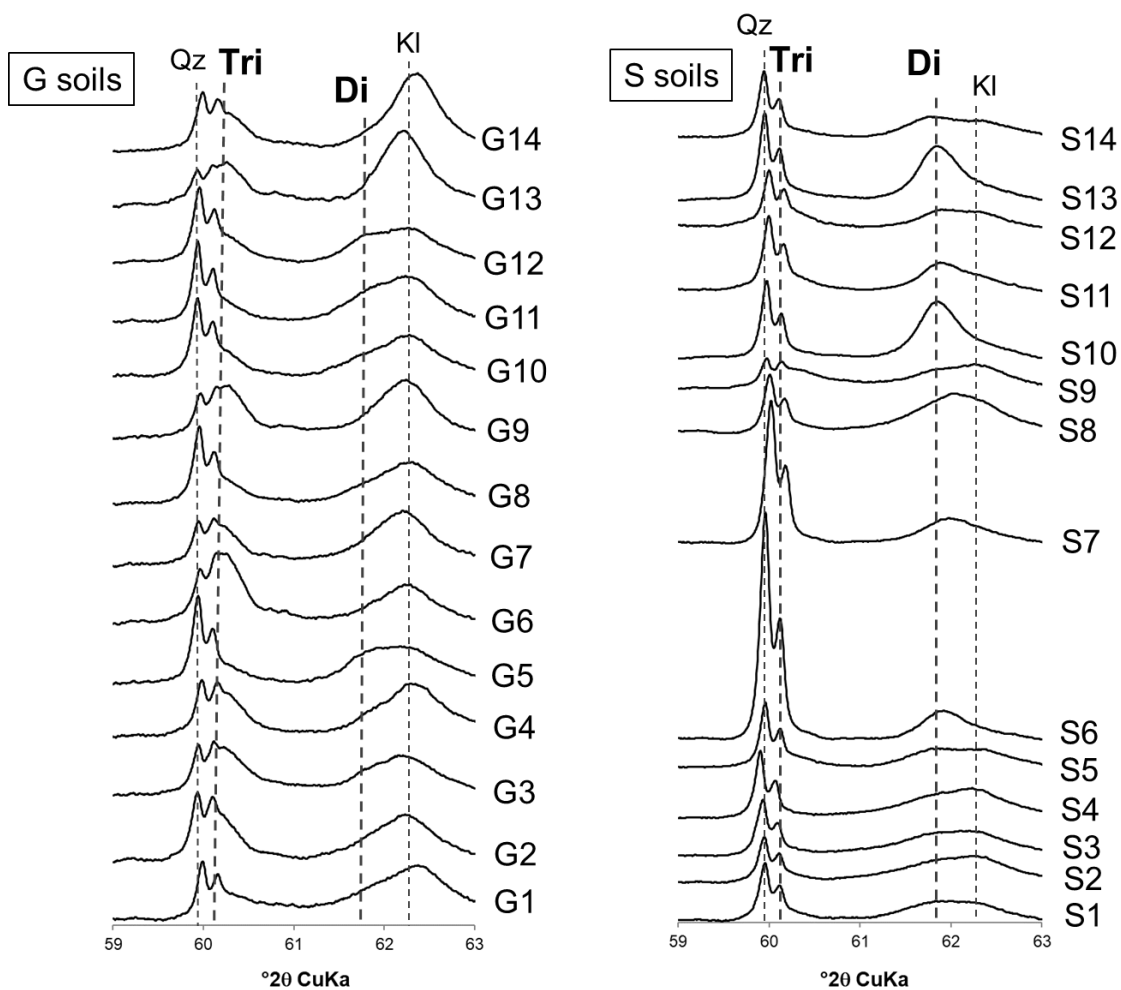




340

341 **Fig. 1** Locations of the soils collected and their surface geology. The geological map  
342 was adopted from 1:20,000 Seamless Digital Geological Map of Japan in Geomap  
343 Navi (<https://gbank.gsj.jp/geonavi/geonavi.php>) by Geological Survey of Japan,  
344 AIST (2014). Authors combined it with blank map downloaded from  
345 (<https://n.freemap.jp/>). The other information including scales, direction, and legends  
346 were added by authors. Detailed legends are available online  
347 ([https://gbank.gsj.jp/seamless/legend\\_e.html](https://gbank.gsj.jp/seamless/legend_e.html)).

348



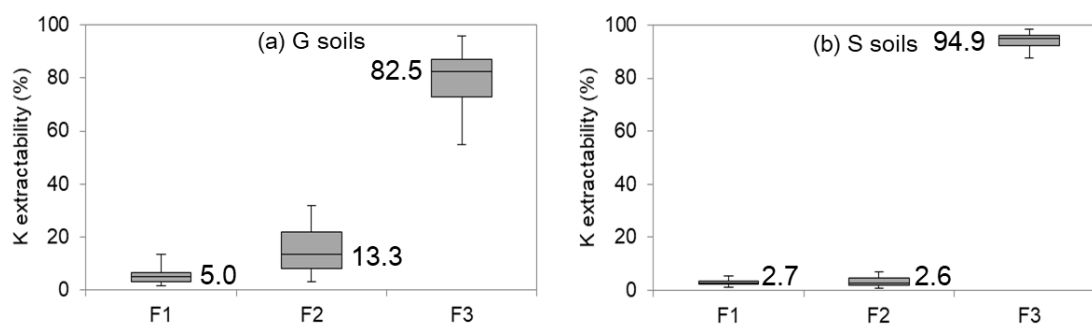
349

350 **Fig. 2** X-ray diffraction patterns for clay-silt fraction collected from soil samples.

351 Abbreviations; Qz: Quartz, Tri: Trioctahedral mineral, Di: Dioctahedral mineral, Kl:

352 Kaolinite

353



354

355 **Fig. 3** The extractability of K for (a) G soils and (b) S soils in each fraction. The grey

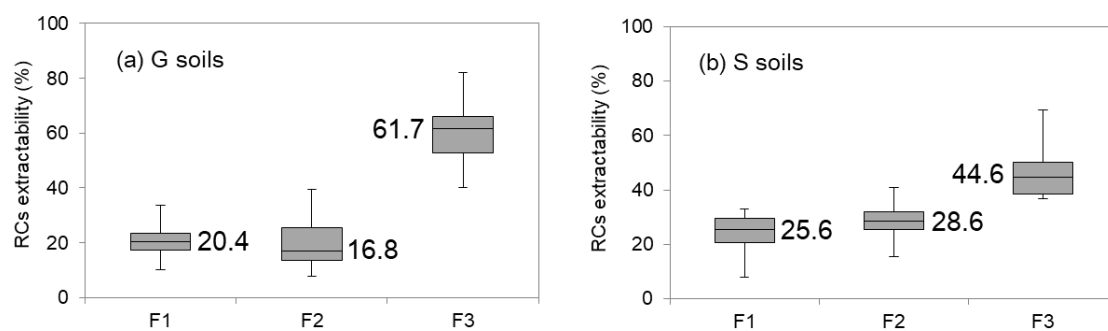
356 colored boxes describe the range of 25–75th percentiles and the horizontal line means

357 the median value. The vertical lines describe the range of maximum and minimum

358 values.

359

360



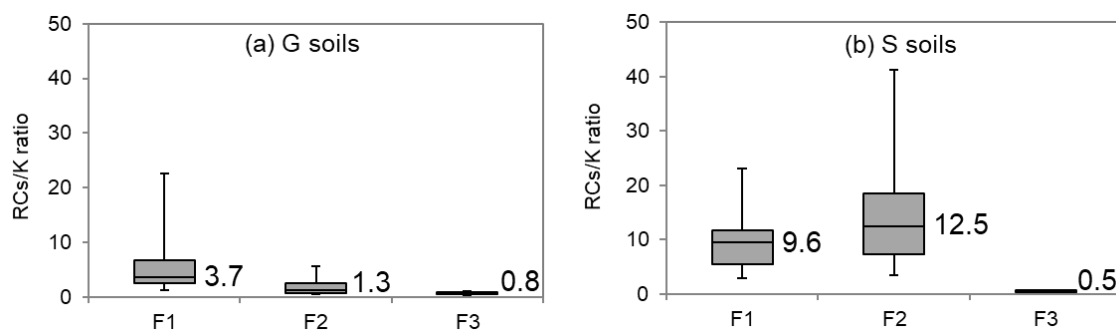
361

362 **Fig. 4** The extractability of RCs for (a) G soils and (b) S soils in each fraction. The grey

363 colored boxes describe the range of 25–75th percentiles and the horizontal line means the

364 median value. The vertical lines describe the range of maximum and minimum values.

365



366

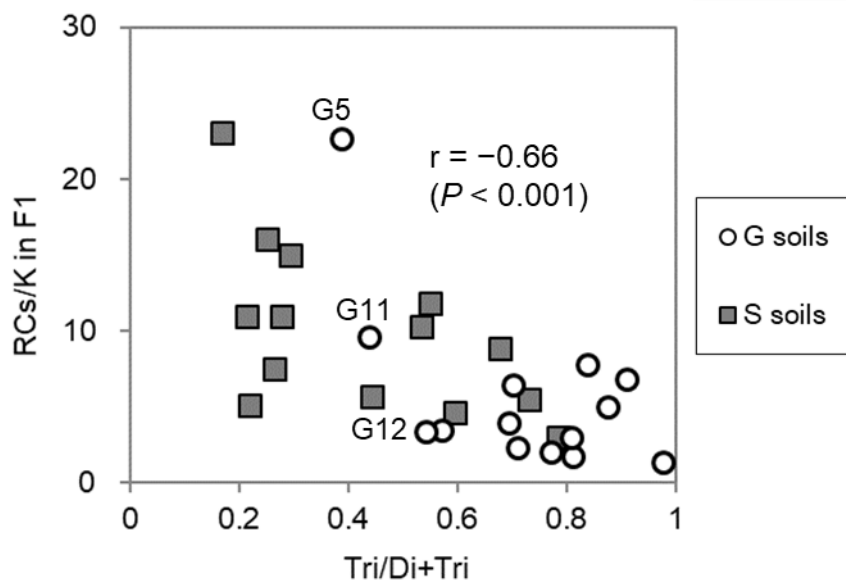
367 **Fig. 5** The ratios of the RCs extractability against that of K for (a) G soils and (b) S

368 soils in each fraction. The grey colored boxes describe the range of 25–75th

369 percentiles and the horizontal line means the median value. The vertical lines

370 describe the range of maximum and minimum values.

371



372

373 **Fig. 6** The relationship between the Tri/Di+Tri and the extractability of RCs against

374 K in F1. (r: Pearson's correlation coefficient)

375